

# A Prototype of a Linear Switched Reluctance Motor with a New Design Methodology

D.S.B. FONSECA

C.P. CABRITA

M.R.A. CALADO

Department of Electromechanical Engineering, CASE-Research Unit on Electrical Drives and Systems  
University of Beira Interior  
Calçada Fonte do Lameiro, P-6201-001 Covilhã  
PORTUGAL  
davide@ubi.pt <http://dem.ubi.pt/~davide>

*Abstract* - A new and original optimized design methodology concerning a Linear Switched Reluctance Machine (LSRM), with a new topology, and to be applied in light electric traction applications, is proposed in this paper. This methodology is based on the systematic use of a simple geometric design process, and a fast simulation methodology is used to evaluate the performance of each one of the several design machines.

*Key-Words* - Linear Switched Reluctance Machines, Traction Forces Evaluation, Machine Simulation, Optimized Design.

## LIST OF SYMBOLS

|                |  |
|----------------|--|
| $B$            | Magnetic flux density  |
| $H$            | Magnetic field intensity                                       |
| $b_p$          | Primary tooth length   |
| $b_s$          | Secondary tooth length   |
| $D_{cu}$       | Winding wire diameter  |
| $F$            | Average value of the developed force                           |
| $g$            | Airgap length  |
| $h_b$          | Coil length  |
| $h_p$          | Primary slot depth   |
| $h_s$          | Secondary tooth depth  |
| $i(x, \psi)$   | Phase instantaneous current                                    |
| $I_{max}$      | Maximum rms value of the coil current                          |
| $I_{pu}$       | Per unit rms current considering $I_{max}$ value as base value |
| $k_e$          | Slot fill factor   |
| $l_b$          | Coil width   |
| $m$            | Primary phase number   |
| $N$            | Number of turns per primary phase                              |
| $N_2$          | Secondary pole number  |
| $N_{db}$       | Number of coils per primary teeth                              |
| $N_{br}$       | Number of coils per winding parallel path                      |
| $N_e$          | Number of turns per primary coil                               |
| $N_r$          | Number of parallel paths of each primary phase                 |
| $U_0$          | DC input voltage of power electronic converter                 |
| $u$            | phase voltage  |
| $v$            | Machine linear speed, or velocity                              |
| $w$            | Primary and secondary stack iron width                         |
| $W_m(x, \psi)$ | Stored magnetic energy   |

|          |  |
|----------|--|
| $x$      | Phase relative position considering the origin on one unaligned position |
| $\tau_p$ | Primary pole pitch   |
| $\tau_s$ | Secondary pole pitch   |
| $\psi$   | Flux linkage   |
| $\eta$   | Expected efficiency  |
| $t$      | Time   |
| $\mu_0$  | Free space magnetic permeability   |

## 1 Introduction

Usually linear machines are employed for straight line displacement applications. Because one wants a traction machine, then the topology shown in Fig. 1 become as a better option, because it presenting a cheap secondary and modular primary construction with articulated mechanical connection between primary phases (movable part) which increases significantly both the fault tolerance and the ability to bend.

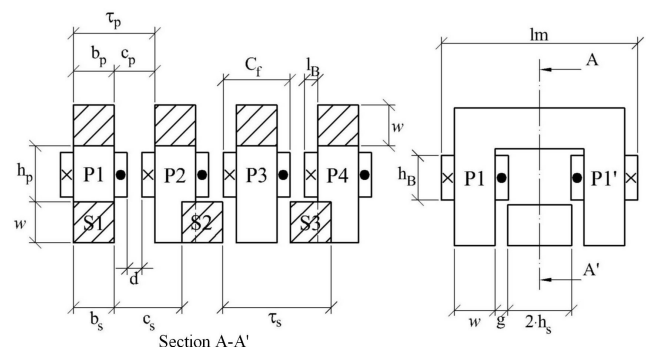


Fig.1 4-phase 8/6 Linear Switched Reluctance Machine geometry and envelope dimensions.

The LSRM optimized design consists to obtain the best performances concerning efficiency and specific power (mechanical output power to the weight ratio). On the other hand, the advantage of a computer simulation for the machine behavior in design process is well defined by T.J.E. Miller [1] “Any switched reluctance motor operates in a series of strokes or transients and does not have a steady-state in which all variables are constant.... This means that for all except the most basic sizing calculations, computer-based design methods must incorporate simulation capability as an integral part of the design process.”

The used simulation methodology is based on the knowledge of the magnetization  $B=f(H)$  characteristic of the used iron material, as well as on the calculated machine dimensions. The simulation methodology permits to obtain the machine magnetization curves based on these values and the linearization of the airgap length mean value between the unaligned and aligned positions [2].

## 2 Geometric design

By application of the Lawrenson's “feasible triangles” presented in Fig. 2, one obtains the following relationship:

$$b_s = C_p = b_p \quad (1)$$

$$\tau_p = b_p + C_p \quad (2)$$

$$\tau_s = b_s + C_s \quad (3)$$

$$C_m = 2m\tau_p = N_2\tau_s \quad (4)$$

$$C_s = \frac{b_p(4m - N_2)}{N_2} \quad (5)$$

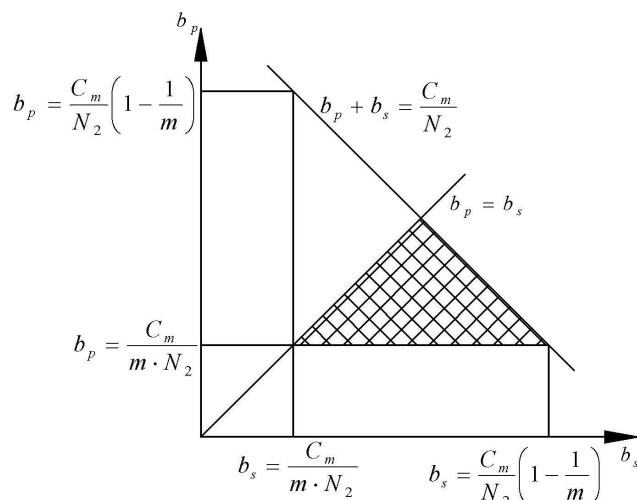


Fig.2 Lawrenson's “feasible triangle” for LSRM.

For rotating SRM is usual to consider the secondary tooth depth  $h_s$  between 20 to 30 times greater than the airgap length  $g$ . However, due to mechanical constraints, the linear machine airgap length must be significantly bigger. Thus,  $h_s$  is equal to 10 to 15 times greater than  $g$  [2], as expressed in (6).

$$h_s = (10 \dots 15)g \quad (6)$$

In this design methodology several combination of the remaining dimensions are explored and one of them is selected to be adopted. Thus, the minimum value of  $b_p$  is limited by maximum operation frequency of the power electronic converter and machine rated speed, and the minimum value of both primary and secondary stack iron width  $w$  is related to the mechanical stress resistance, namely because of the attraction forces between primary and secondary. In this prototype one have consider 18mm as the minimum value of both  $b_p$  and  $w$ .

As shown in [2] the control strategy adopted to be used at the continuous rated regime is a single pulse operation with the turn on position equal to zero and commutation position equal to 40% of the secondary pole pitch.

To analyze  $w$ ,  $b_p$ ,  $g$  and  $N_e$  (number of turns per coil) and their influence on the machine performance, the winding wire diameter  $D_{cu}$  was chosen with the standard value of 0.5mm. Thus, the maximum rms value for the coil current is given by:

$$I_{max} = \frac{D_{cu}^2 \cdot 3.5 \cdot 10^6 \cdot \pi}{4} \quad (7)$$

Once the desired machine is a 600W machine and that  $I_{max}$  is approximately 0.7A, then the phase winding must be composed by 4 coil parallel connected.

For simulation purpose the coil resistance is calculated according to the following relation:

$$R_{coil} = \frac{4\rho N_e}{\pi D_{cu}^2} [2.2w + 0.9\pi(b_p + l_B)] \quad (8)$$

were  $l_B$  is according to the following relationship:

$$A_B = N_e \cdot N_{bd} \frac{\pi d_{cu}^2}{4k_e} = l_B h_B \quad (9)$$

where the slot fill factor  $k_e$  is usually of the order of 0.4 for concentrated windings.

In addition, to avoid a large leakage flux, the following relationships should be respected:

$$l_B \leq 1.3w \quad (10)$$

and

$$l_B \leq 1.3b_p \quad (11)$$

### 3 Simulation methodology

For machine simulation one considers that all phase coils are series-connected, and the DC input voltage for power electronic energy converter is given by the following equation:

$$U = N_r U_o \quad (12)$$

Independently of the chosen inverter topology, by application of the 2nd Kirchhoff's law one obtains the following time dependent equation for an excited phase circuit:

$$u(t) = R i(t) + \frac{\partial \psi(t)}{\partial t} \quad (13)$$

where  $R$  is the equivalent phase resistance given by:

$$R = N_r \cdot N_{br} \cdot R_{coil} \quad (14)$$

If one consider a constant linear speed  $v$ , then (13) can be rewritten as follows:

$$\frac{\partial \psi}{\partial x} = \frac{V(x) - R \cdot I(x, \psi)}{v} \quad (15)$$

Thus, knowing position, current and flux linkage values for a position  $x_n$ , and applying the Runge-Kutta method to (15), and considering a step of  $\Delta x$ , one obtains:

$$\psi(x_{n+1}) = \psi(x_n) + \Delta \psi(x_n) \quad (16)$$

$$\Delta \psi(x_n) = \frac{[K_1(x_n) + 2K_2(x_n) + 2K_3(x_n) + K_4(x_n)]}{6} \quad (17)$$

$$K_1(x_n) = \frac{u(x_n) - R \cdot i[x_n, \psi(x_n)]}{v} \cdot \Delta x \quad (18)$$

$$K_2(x_n) = \frac{\Delta x}{v} \left[ u(x_n) - \right. \quad (19)$$

$$\left. - R \cdot i \left[ \left( x_n + \frac{\Delta x}{2} \right), \left( \psi(x_n) + \frac{K_1(x_n)}{2} \right) \right] \right]$$

$$K_3(x_n) = \frac{\Delta x}{v} \left[ u(x_n) - \right. \quad (20)$$

$$\left. - R \cdot i \left[ \left( x_n + \frac{\Delta x}{2} \right), \left( \psi(x_n) + \frac{K_2(x_n)}{2} \right) \right] \right]$$

$$K_4(x_n) = \frac{\Delta x}{v} \left[ u(x_n) - \right. \quad (21)$$

$$\left. - R \cdot i \left[ (x_n + \Delta x), (\psi(x_n) + K_3(x_n)) \right] \right]$$

Taking into account that the exposed method uses both the flux linkage and relative position as state variables, the developed force is derived from D'Lambert's principle as follows [3]:

$$f(x, \psi) = - \left. \frac{\partial W_m(x, \psi)}{\partial x} \right|_{\psi=\psi_j} \quad (22)$$

$$f(x, \psi) = \frac{W_m[(x - \Delta x), \psi] - W_m[(x + \Delta x), \psi]}{2 \cdot \Delta x} \quad (23)$$

where  $\Delta x$  should tend to zero and must be lower than  $x_n$ , and the phase stored magnetic energy  $W_m$  is obtained by the following relationship:

$$W_m(x, \psi_j) = \int_{\psi=0}^{\psi=\psi_j} i(x, \psi) \partial \psi \Big|_{x=Const.} \quad (24)$$

As can be seen, several values for current  $i(x, \psi)$  and force  $W_m(x, \psi)$  are necessary being calculated by using the magnetization curves lookup table. The necessary values obtained directly from a lookup table, are obtained from numerical interpolation using Cubic Spline Interpolation.

### 4 Magnetization curves

As explained, this simulation method requires the use of a lookup table representative of the magnetization curves.

For exact determination of the machine magnetization curves based on its dimensions there are two possible ways:

- from finite element analysis
- from static test measurements [4]

In this work the used methodology to obtain the magnetization curves is presented in [5] and is made through the linearization of the airgap length mean value between the unaligned and aligned positions.

According to [5] and considering all series-connected phase coils, the following equations represent a simplest and fast method to obtain  $\psi$  from  $B-H$  characteristic represented in Fig. 3:

$$\psi = N B w b_p, \quad (25)$$

where  $N$  is the number of turns per phase, given by:

$$N = N_r N_{br} N_e \quad (26)$$

Then, the input coil current for each relative position is obtained by using the following equation:

$$I(x, \psi) = \frac{H l_f(x) + \frac{\psi l_g(x)}{N w b_p \mu_0}}{N} \quad (27)$$

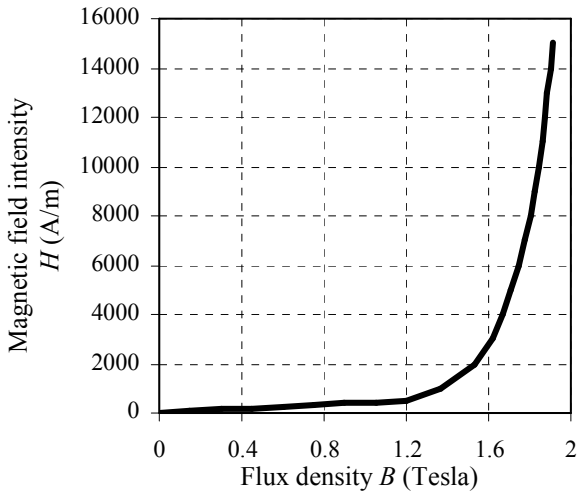


Fig.3 Magnetization curves for the magnetic circuit material.

where  $l_g$  and  $l_f$  are respectively the airgap and iron average lengths of flux path, for each position, and are given by the following equations, if  $0 < x < 0.5\tau_s$ :

$$l_g(x) = 2(g + h_s) - \frac{4h_s x}{\tau_s} \quad (28)$$

$$l_f(x) = 2(h_p + 2(g + h_s + w)) - l_g(x) \quad (29)$$

Fig. 4 illustrates the airgap average length of flux path versus relative position characteristic, considering  $g=3\text{mm}$  and  $b_p = 18\text{mm}$ . Note that both  $x = 0$  and  $x = \tau_s$  are unaligned positions, whereas  $x = 0.5\tau_s$  is the aligned position.

In addition, Fig. 5 shows, for exemplification purposes, the magnetization characteristics of the future selected prototype. As can be seen, the lookup table values of the magnetization characteristics are stored in the form of necessary current in a phase to achieve a specific value of linkage flux for a given position.

Airgap average length of flux path versus relative position characteristic

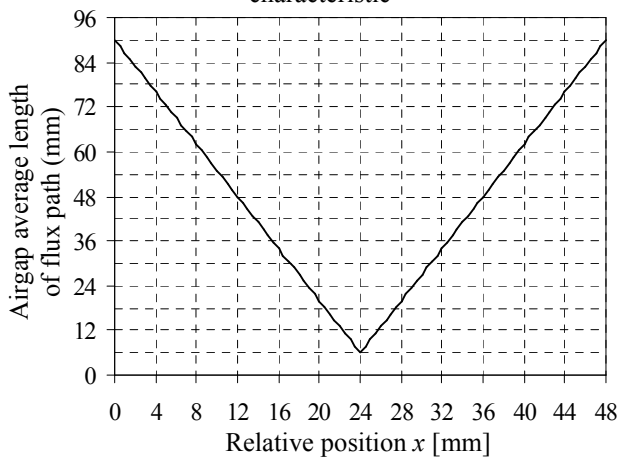


Fig.4 Airgap average length versus relative position.

Graphic representation of the machine magnetization curves lookup table

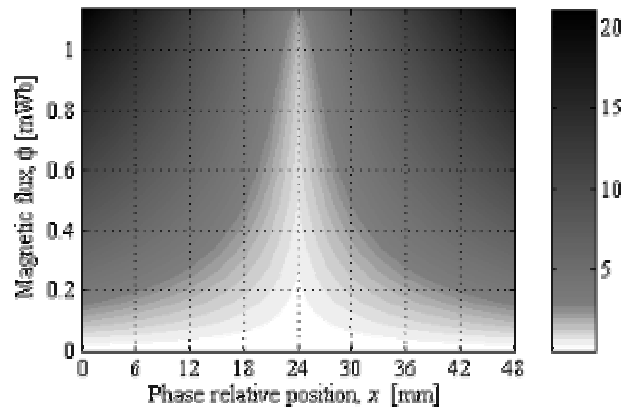


Fig.5 Phase current [A] versus relative position and flux linkage (magnetization curves).

Graphic representation of the stored magnetic energy,  $W_m$ , concerning one phase magnetic circuit

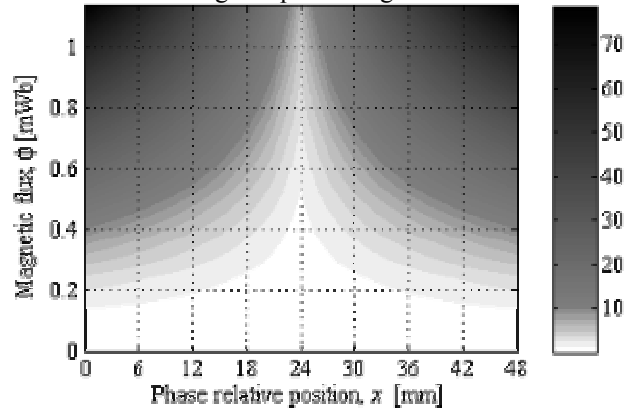


Fig.6 Stored magnetic energy [Joule] versus relative position and flux linkage, for one machine phase.

## 5 Design results

As an example a prototype was designed with the following requirements:

- rated speed: 10 m/s
- developed force at rated speed: 60N
- supply voltage: 200V

For this design analysis the airgap was set in steps of 1mm and the primary teeth length was set in steps of 3mm in order to obtain measurable values of the secondary pole pitch.

The winding wire diameter  $D_{cu}$  was chosen with the standard value of 0.5mm, and as seen before, each phase winding is composed by 4 coil parallel connected, thus  $N_r = 4$ .

The number of turns per coil was set in steps of 80 because one wants to use this prototype for fault tests.

It can be seen in Fig. 7, where all machines with insufficient force or with high current are not display for clearly, that the  $b_p$  and  $g$  must be as smaller as possible in order to maximize efficiency.

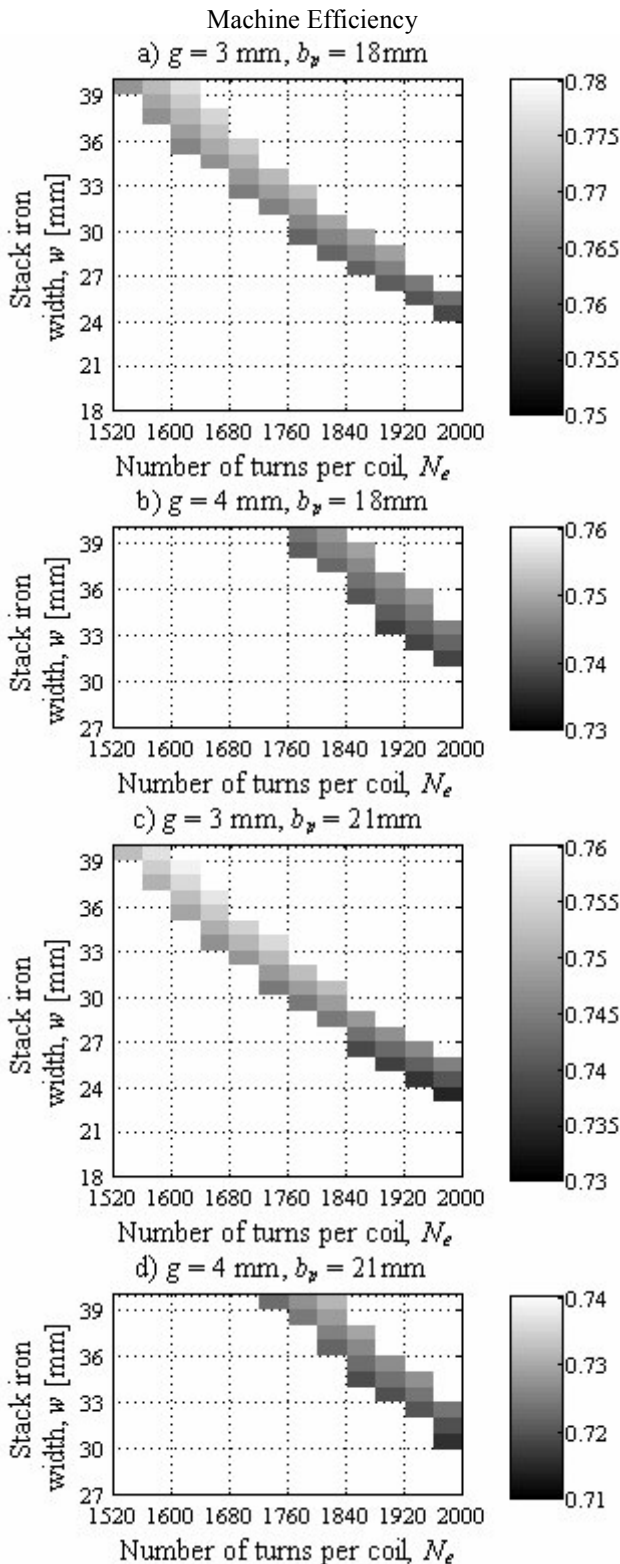


Fig.7 Machine efficiency as a function of  $N_e$  and  $w$  for several combinations of  $g$  and  $b_p$ .

In addition, Fig. 8 shows the influence of both  $N_e$  and  $w$ , considering the selected values of 3mm and 18mm for  $g$  and  $b_p$  respectively, in the most significant remaining machine dimension, the machine height, and on the machine developed force,

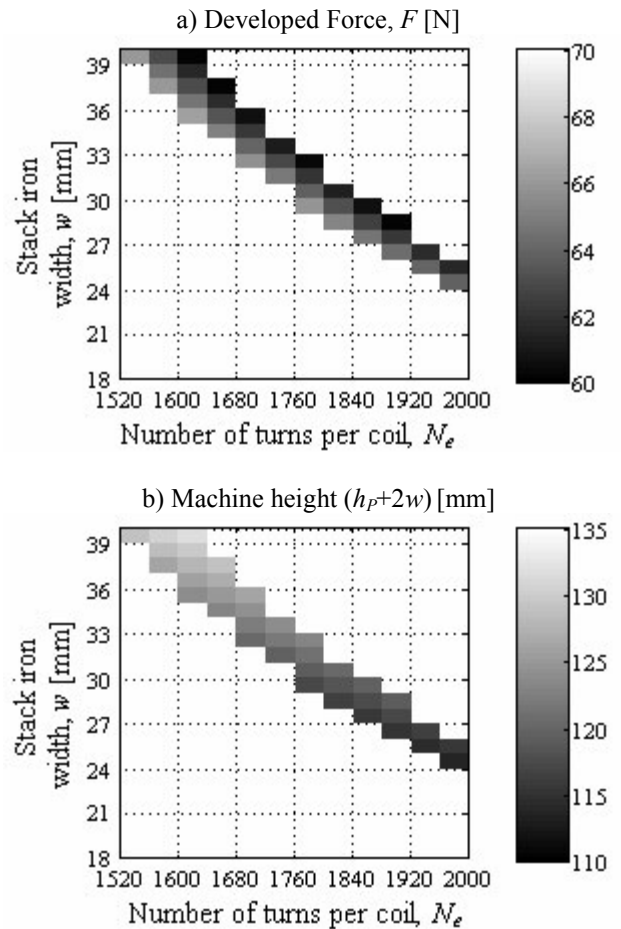


Fig.8 Influence of  $N_e$  and  $w$  on the machine dimensions and performance.

the last the most important of the remaining performance parameters.

In authors' opinion, the most suitable machine for selected traction application should have the following dimensions:

- $b_p=18\text{mm}$
- $g=3\text{mm}$
- $w=33\text{mm}$
- $N_e=1680$  turns

In order to evaluate if the selected  $D_{cu}$  value is the most suitable, Table 1 and Table 2 presents several winding configurations.

Note that, for the same slot fill factor and current density in the copper, independently from  $D_{cu}$ , the necessary winding develop similar force with similar efficiency.

## 6 Conclusions and future work

The proposed methodology, concerning LSRM design, is a good contribution and a strong advantage. This method is faster than others based on finite element method and more accurate than analytic

Table 1 Different winding topologies for the prototype, as a function of some dimensional characteristics.

|       | slot fill factor, $K_e$ [%] |       |       | Number of turns per primary coil, $N_e$ |      |      |
|-------|-----------------------------|-------|-------|---|------|------|
|       | $D_{cu}$ [mm]               |       |       | $D_{cu}$ [mm]                           |      |      |
| $N_r$ | 0.2                         | 0.5   | 0.8   | 0.2                                     | 0.5  | 0.8  |
| 1     | 7.95                        | 24.11 | 40.38 | 6680                                    | 3240 | 2120 |
| 2     | 12.38                       | 35.12 | 48.76 | 5200                                    | 2360 | 1280 |
| 4     | 18.67                       | 50.00 |       | 3920                                    | 1680 | 640  |
| 6     | 23.71                       |       |       | 3320                                    |      |      |
| 22    | 48.19                       |       |       | 1840                                    |      |      |
| 24    | 48.00                       |       |       | 1680                                    |      |      |

Table 2 Different winding topologies for the prototype, and influence on the machine performance.

|       | $I_{pu}$      |       |       | Efficiency, $\eta$ [%] |       |       | Force, $F$ [N] |       |       |
|-------|---------------|-------|-------|------------------------|-------|-------|----------------|-------|-------|
|       | $D_{cu}$ [mm] |       |       | $D_{cu}$ [mm]          |       |       | $D_{cu}$ [mm]  |       |       |
| $N_r$ | 0.2           | 0.5   | 0.8   | 0.2                    | 0.5   | 0.8   | 0.2            | 0.5   | 0.8   |
| 1     | 0.905         | 0.911 | 0.916 | 34.57                  | 62.49 | 73.05 | 1.44           | 13.93 | 38.37 |
| 2     | 0.906         | 0.925 | 1.132 | 46.13                  | 70.40 | 76.85 | 3.65           | 29.88 | 86.73 |
| 4     | 0.912         | 0.962 |       | 56.51                  | 76.78 |       | 8.43           | 63.91 |       |
| 6     | 0.901         |       |       | 62.12                  |       |       | 13.18          |       |       |
| 22    | 0.907         |       |       | 76.17                  |       |       | 52.91          |       |       |
| 24    | 0.997         |       |       | 76.10                  |       |       | 63.42          |       |       |

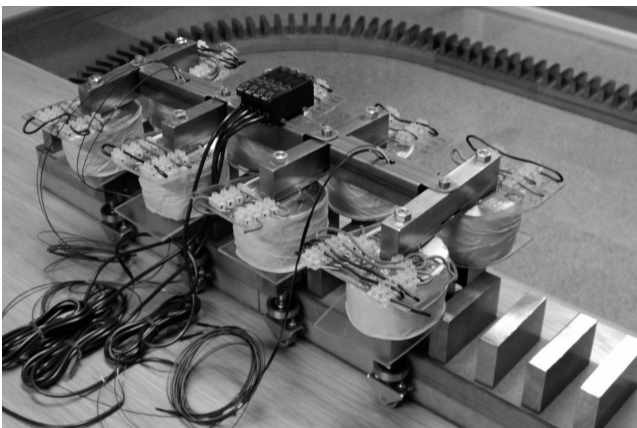


Fig.9 General view of the LSRM prototype.

design. It saves engineering costs, producing also good approximations at first attempt, and provides convenient learning and simulation facilities.

#### Acknowledgments

The authors would like to thank the financial support provided by the University of Beira Interior and the CASE-Centro de Accionamentos e Sistemas Eléctricos da Fundação para a Ciência e a Tecnologia (FCT) of Portugal.

#### References:

- [1] T. J.E. Miller, *Switched Reluctance Motors and their Control*, Oxford, UK: Magna Physics Publishing and Clarendon Press, 1993.
- [2] D. S. B. Fonseca, C. P. Cabrita, M. R. A. Calado, Linear Switched Reluctance Motor. A new Topology for Fault Tolerant Traction Applications, *Proceedings of the 2005 IEEE International Electric Machines and Drives Conference IEMDC'2005, San Antonio, Texas, USA, May 15-18, 2005*, pp. 823-827.
- [3] Nicholas J. Nagel and Robert D. Lorenz, Modelling of a Saturated Switched-Reluctance Motor Using an Operating Point Analysis and the Unsaturated Torque Equation, *IEEE Trans. on Industry Applications*, Vol. 36, No. 3, May/June 2000, pp. 714-722.
- [4] C. Cossar and T.J.E. Miller, Electromagnetic Testing of Switched Reluctance Motors, *Proceedings of the International Conference on Electrical Machines ICEM'92*, Manchester, UK, September 14-17, 1992, pp. 470-474.
- [5] Fonseca, D. S. B., Cabrita, C. P., Calado, M. R. A. Linear Switched Reluctance Motor. A New Design Methodology Based on Performance Evaluation, *IEEE International Conference on Industrial Technology ICIT'2004, Yasmine, Hammamet, Tunisia, December 8-10, 2004*, paper TF-001696.